The Sca-1 cell surface marker enriches for a prostate-regenerating cell subpopulation that can initiate prostate tumorigenesis

Li Xin*†, Devon A. Lawson*†, and Owen N. Witte*‡§

Departments of *Microbiology, Immunology, and Molecular Genetics and ‡Molecular and Medical Pharmacology, David Geffen School of Medicine, and Howard Hughes Medical Institute, University of California, Los Angeles, CA 90095

Contributed by Owen N. Witte, March 22, 2005

Sca-1 (stem cell antigen-1) enriches for murine prostate cells capable of regenerating tubular structures containing basal and luminal cell lineages in a dissociated cell prostate regeneration system. Sca-1$^+$ fractions are enriched for cells at the G_0 stage of the cell cycle, and Sca-1$^+$ cells cluster in the proximal region of prostatic tubules where replication-quiescent cells have been localized. Castration-induced enrichment for androgen-independent cells results in a concomitant enrichment for Sca-1$^+$ cells. Genetic perturbations of PTEN/AKT signaling in prostate-regenerating cells leads to the initiation of tumorigenesis, and cancer progression is associated with a dramatic increase in Sca-1$^+$ cells. Sca-1-enriched prostate-regenerating cells possess multiple stem/progenitor cell properties and can serve as targets for cancer initiation.

AKT | prostate cancer | PTEN | stem cell

The properties shared by cancer and stem cells have led to a model for tumorigenesis where the target for transformation is the somatic stem cell or differentiated cell types that have reacquired the ability for self-renewal (1, 2). Tumor cells and tissue stem cells exploit many of the same pathways, such as Wnt and Sonic hedgehog, to give them the capacity for extensive proliferation and self-renewal (3, 4). Small subpopulations of cancer cells have been shown to be capable of initiating and sustaining tumor growth when transplanted into immune-deficient mice (5–7).

The prostate contains classes of epithelial cells with variable differentiation status that may serve as targets for tumor initiation (8–10). Androgen cycling experiments suggest that stem cell activity is present in the prostate (11). These cells are thought to reside in the basal layer of the prostate because these cells are androgen-independent and preferentially retained in castrated rodents. Stem cells in the basal layer give rise to transit-amplifying epithelial cells (TACs) that differentiate to produce terminally differentiated secretory luminal cells (12).

The most common form of human prostate cancer expresses luminal cell-specific markers (cytokeratins 8 and 18 and prostate-specific antigen) but low levels of the basal cell marker (p63), suggesting that the disease originates in terminally differentiated luminal cells (12, 13). Some studies suggest that the disease is derived from high-grade prostatic intraepithelial neoplasia (PIN), which is believed to arise from intermediate epithelial cells (14). Other studies demonstrate that the majority of androgen-independent tumors express genes such as bcl-2 that are characteristic of the basal/stem cell compartment in normal prostate tissue (8). Prostate cancers may arise from stem cells that undergo aberrant proliferation and differentiation to produce a heterogeneous population of cells expressing luminal-, basal-, and intermediate cell-specific genes (14, 15).

The tissue recombination procedure developed by Cunha and Lung (16) uses fragments dissected from rat or mouse urogenital sinus mesenchyme (UGSM) in combination with adult epithelial tissue to regenerate prostate-like tissues. We developed a dissociated cell system to facilitate the study of unique prostate cell subpopulations to demonstrate that a subpopulation of murine prostate cells possesses stem-like capacity for *de novo* tubule regeneration (17). We find that Sca-1 (stem cell antigen-1), a glycosylphosphatidylinositol-linked cell surface protein known to enrich for somatic stem cells in other tissues (18, 19), can be used to enrich for prostate-regenerating cells (PRCs). Sca-1$^+$ cell fractions contain an increased percentage of cells with immature cell properties, including replication quiescence, androgen independence, and multilineage differentiation potential. Perturbations of the PTEN/AKT signaling axis in these cells result in the initiation of prostate tumorigenesis, and cancer progression is associated with a concomitant increase in Sca-1$^+$ cells. These studies suggest that Sca-1-enriched PRCs possess multiple stem/progenitor cell properties and can serve as targets for the initiation of prostate tumorigenesis.

Materials and Methods

Infection of Dissociated Prostate Cells with Lentivirus and Prostate Regeneration. β-Actin GFP transgenic mice were purchased from The Jackson Laboratory [C57BL/6-TgN(ACTbEGFP)1Osb]. Dissociated prostate cells were prepared from 6- to 10-week-old C57BL/6 and β-actin GFP transgenic mice as described in ref. 17. Lentivirus preparation, titering, and infection of dissociated prostate cells were performed as described in ref. 17. Surgical procedures for prostate regeneration were also performed as described in ref. 17.

FACS Analysis. Dissociated prostate cells were stained with FITC-conjugated anti-Sca-1 antibody (1 μM final concentration, Pharmingen) or FITC-conjugated rat IgG2a isotype control (1 μM final concentration, Pharmingen). Cell cycle analysis was performed on prostate cells sorted magnetically based on Sca-1 expression according to the protocol described in ref. 20. Briefly, cells were resuspended in 0.5 ml of NASS buffer (0.15 M NaCl/5 mM sodium EDTA/0.5% BSA fraction V/0.1 M phosphate-citrate buffer, pH 4.8) containing 0.02% saponin and 10 μg/ml 7-aminoactinomycin D at room temperature for 20 min. Cells were washed with 1× PBS and resuspended in NASS containing 0.02% saponin and 10 μg/ml actinomycin D at 4°C for 5 min. A half-microliter of 1 μg/ml pyronin Y diluted in distilled water was added, and samples were incubated at 4°C for 10 min before FACS analysis.

Freely available online through the PNAS open access option.

Abbreviations: TAC, transit-amplifying epithelial cell; UGSM, urogenital sinus mesenchyme; PRC, prostate-regenerating cell; moi, multiplicity of infection; PIN, prostatic intraepithelial neoplasia; mPIN, mouse PIN; SCID, severe combined immunodeficient; AR, androgen receptor; H&E, hematoxylin/eosin; PI, propidium iodide.

†L.X. and D.A.L. contributed equally to this work.

§To whom correspondence should be addressed at: Howard Hughes Medical Institute, University of California, 675 Charles E. Young Drive South, 5-748 MRL, Los Angeles, CA 90095-1662. E-mail: owenw@microbio.ucla.edu.

Magnetic Bead Sorting. Dissociated prostate cells were incubated with biotinylated anti-Sca-1 antibody (1 μM final concentration, eBioscience, San Diego) in 1 ml of DMEM/10% FBS for 20 min at 4°C. Cells were pelleted, washed, and incubated with CELLection Biotin Binder Dynabeads (1×10^7 beads per ml final concentration, Dynal Biotech, Brown Deer, WI) at 4°C for 20 min and placed in a magnetic particle separator (Dynal Biotech) for 1 min. Unbound (Sca-1$^-$) fractions were collected, and bound (Sca-1$^+$) fractions were incubated in DNase I buffer for 15 min at 37°C for cleavage of oligonucleotide linkers to release cells from beads. Light microscope analysis showed that <1% of cell suspensions contained small clumps both before and after fractionation. Cells were counted by hemocytometer.

Fluorescent Imaging. CB.17$^{SCID/SCID}$ mice bearing prostate tissue grafts were killed 6–10 weeks after surgery. Kidneys were placed in a light-tight chamber equipped with a halogen light source, and images were acquired for 1 s by using the IVIS optical imaging system (Xenogen, Alameda, CA). Regions of interest were drawn around grafts, and fluorescent signal was quantified by using LIVING IMAGE SOFTWARE 2.20 (Xenogen).

Histological, Immunohistochemical, and Immunofluorescent Analysis. Histological and immunohistochemical analysis were performed as described in ref. 17. Paraffin-embedded sections were stained with hematoxylin/eosin (H&E) or polyclonal rabbit anti-AR (1:200 dilution, Santa Cruz Biotechnology), monoclonal antibody against p63 (4A4, 1:150, Santa Cruz Biotechnology) and polyclonal rabbit anti-phospho-Akt (Ser 473, 1:200, Cell Signaling Technology, Beverly, MA). For visualization of GFP, frozen sections were air-dried, fixed in 5% paraformaldehyde, and mounted in mounting medium containing propidium iodide (PI) (Vector Laboratories). For Sca-1 fluorescent staining, longitudinal frozen sections were stained with rat monoclonal anti-Sca-1 (1:250, Pharmingen), incubated with a biotin-conjugated rabbit anti-rat antibody (1:200, DakoCytomation, Carpinteria, CA), and incubated with FITC-conjugated streptavidin (1:200, Jackson ImmunoResearch). Sections were counterstained with PI in mounting medium and analyzed by fluorescent microscopy.

Results

The Sca-1 Cell Surface Protein Enriches for Bipotent Murine Prostate Cells with Prostate-Regenerating Activity. To enrich for PRCs, we compared the ability of various cell surface markers to enrich for cells with prostate-regenerating activity. Sca-1, a member of the Ly-6 family of glycosylphosphatidylinositol-linked proteins, has been used as a marker to enrich for hematopoietic and mammary gland stem cells (18, 19). FACS analysis indicates that ≈15% of prostate cells dissociated from 8-week-old adult C57BL/6 mice express the Sca-1 surface protein. Less than 3% of Sca-1$^+$ prostate cells are CD45$^+$, suggesting that they are not infiltrating hematopoietic cells (data not shown).

Single cell suspensions from 8-week-old murine prostate were separated into Sca-1$^+$ and Sca-1$^-$ fractions by using magnetic bead sorting as described in *Materials and Methods* to compare the regenerative activity of each subpopulation. FACS and RT-PCR analyses of Sca-1$^+$ and Sca-1$^-$ fractions demonstrate that a 3- to 5-fold enrichment for Sca-1$^+$ cells is achieved by using this sorting technique (Fig. 5, which is published as supporting information on the PNAS web site). Single Sca-1-enriched or Sca-1-depleted cells (1×10^5) were mixed with an equal number of UGSM cells and implanted under the kidney capsule of severe combined immunodeficient (SCID) mice. Transillumination microscopy images (Fig. 1*A Upper*) demonstrate that grafts regenerated from Sca-1$^+$ cell fractions are significantly larger than grafts regenerated from Sca-1$^-$ cell fractions. Tissue sections from Sca-1$^+$ grafts are larger in average area and contain more prostatic tubule structures than do tissue sections from Sca-1$^-$ grafts (Fig. 1*A Lower*). Sca-1$^+$ grafts also weigh more on average than Sca-1$^-$ grafts (44 mg vs. 7 mg, respectively). Therefore, enrichment for cells expressing the Sca-1 marker results in an enrichment for cells with prostate-regenerating activity.

To determine whether individual tubules are derived from a single cell or from the combined action of many cells, dissociated cell suspensions were prepared from prostate tissue from C57BL/6 mice and β-actin GFP transgenic mice (Fig. 1*B*). Dissociated cells from β-actin GFP mice were separated into Sca-1$^+$ and Sca-1$^-$ fractions by using magnetic beads. Sca-1$^+$GFP$^+$ or Sca-1$^-$GFP$^+$ cells (5×10^4) were mixed with 5×10^4 cells from C57BL/6 mice and 1×10^5 UGSM cells and put into the regeneration system for 10 weeks. Analysis of representative grafts by fluorescence microscopy and charge-coupled device camera shows the presence of 4–5 times more GFP in grafts regenerated from Sca-1$^+$ fractions than Sca-1$^-$ fractions. Fluorescence images of tissue sections representing multiple positions along regenerated tubules demonstrate the presence of more GFP$^+$ cells in grafts grown from Sca-1$^+$ cells than from Sca-1$^-$ cells (Fig. 1*B*), confirming that the Sca-1 antigen can enrich for PRCs. High-power analysis of tissue sections indicates that each tubule is composed entirely of either GFP-expressing or non-GFP-expressing cells (Fig. 1*C*). Even GFP$^+$ tubules that appear to contain some cells lacking GFP signal express the protein when viewed by confocal microscopy (Fig. 1*C Right*). The lack of chimeric tubules containing both GFP$^+$ and GFP$^-$ cells shows that single Sca-1-enriched PRCs can give rise to whole tubular structures.

Androgen receptor (AR), p63, and synaptophysin have been used as the markers for basal, luminal, and neuroendocrine cell lineages, respectively (9, 13). To determine whether regenerated tubules contain multiple cell lineages, we performed immunohistochemical analysis to check for the expression of these proteins in tissue sections from Sca-1$^+$ grafts. Our results demonstrate that each tubule contains both AR-positive luminal cells and p63$^+$ basal cells (Fig. 1*D*). Neuroendocrine cells could not be identified by staining for synaptophysin (data not shown). Because each tubule structure appears to be derived from a single cell, the presence of both basal and luminal cell lineages in each tubule suggests that the Sca-1-enriched PRCs are at least bipotent.

Sca-1$^+$ Cells Are Largely Replication-Quiescent and Androgen-Independent and Cluster in the Proximal Region of Murine Prostatic Tubules. To determine whether Sca-1$^+$ cell fractions are enriched for replication-quiescent cells, prostate cells were obtained from 8-week-old C57BL/6 mice and fractionated based on Sca-1 expression by using magnetic bead sorting. Sca-1$^+$ and Sca-1$^-$ fractions were stained with 7-aminoactinomycin D to measure DNA content and stained with pyronin Y to measure RNA content by using a previously established protocol (20). FACS analysis demonstrates that Sca-1$^+$ cell fractions contain nearly 2-fold more cells in the G_0 phase of the cell cycle as defined by both low RNA and DNA staining (Fig. 2*A*). Sca-1$^+$ cell fractions also contain two to three times fewer cells in the G_1 phase than Sca-1$^-$ fractions. Interestingly, 3-fold more Sca-1$^+$ cells appear to be in the division phases ($S/G_2/M$) of the cell cycle than Sca-1$^-$ cells. Prostate cell fractions sorted by several other markers did not differ in cell cycle status (data not shown). These data suggest that Sca-1$^+$ cell fractions contain higher percentages of both replication-quiescent and actively dividing cells.

BrdUrd label retention strategies have identified replication-quiescent stem-like cells in the murine prostate concentrated in the proximal regions of prostatic tubules near the urethra (21). The proximal and distal regions of the anterior, ventral, and dorsolateral lobes were microdissected from 8-week-old mice as illustrated in Fig. 2*B*. FACS analysis demonstrates that 29% of cells in the proximal regions of prostatic tubules express Sca-1,

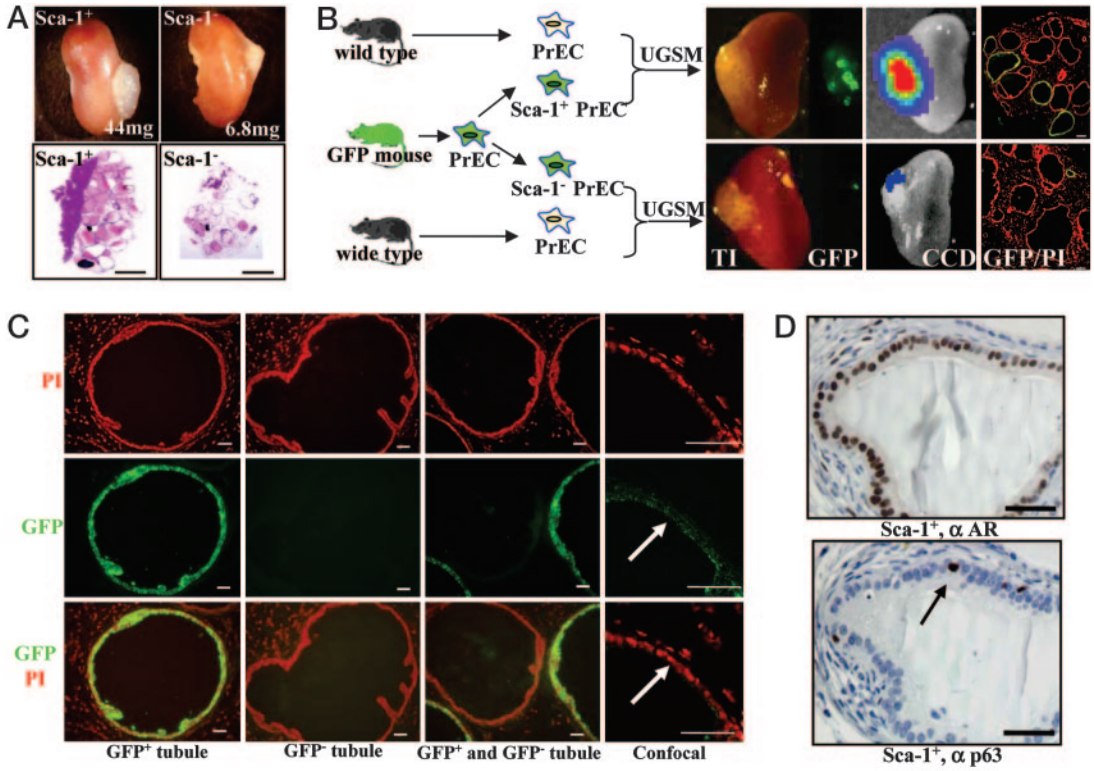

Fig. 1. Sca-1 enriches for cells with prostate-regenerating activity. (*A*) Comparison of regenerative activity of Sca-1$^+$ and Sca-1$^-$ prostate cell fractions. Single cell suspensions prepared from 8- to 10-week-old murine prostate tissue were separated into Sca-1$^+$ and Sca-1$^-$ fractions by using magnetic bead sorting. Sca-1$^+$ or Sca-1$^-$ cells (1×10^5) were combined with 1×10^5 UGSM cells. Regenerated grafts were harvested 10 weeks later, and regenerative activity was compared by transillumination microscopy (*Upper*) and H&E staining of tissue sections (*Lower*). Original magnification of H&E staining: ×10. (Scale bars, 100 μm.) (*B*) Strategy for investigation of differentiation potential of Sca-1-enriched PRCs. Dissociated prostate epithelial cells were prepared from 8-week-old C57BL/6 mice and β-actin GFP transgenic mice, as shown schematically. Cells from β-actin GFP mice were sorted into Sca-1$^+$ and Sca-1$^-$ fractions by using magnetic beads. Sca-1$^+$GFP$^+$ or Sca-1$^-$GFP$^+$ prostatic epithelial cells (5×10^4) were mixed with 5×10^4 cells from C57BL/6 mice and 1×10^5 UGSM cells and incubated under the kidney capsule of SCID mice. Transillumination (TI) and fluorescent (GFP) images were taken of grafts harvested after a 10-week incubation. GFP signal from each graft was quantified by using a charge-coupled device camera. Frozen tissue sections were counterstained with PI and analyzed by fluorescence microscopy. Original magnification: ×40 (Scale bars, 100 μm.) (*C*) Single Sca-1-enriched PRCs can regenerate prostatic tubular structures. High-magnification fluorescent images of tissue sections from chimeric tissue grafts show that each prostatic tubule consists exclusively of single donor cell type. Confocal microscopy analysis of sections reveals fluorescence at sites within GFP$^+$ tubules where GFP expression is low. Original magnification: ×100. (Scale bars, 100 μm.) (*D*) Sca-1-enriched PRCs can give rise to both basal and luminal cells. Paraffin sections were prepared from each graft and stained with antibodies against p63 (arrow) and the AR as described in *Materials and Methods.* Original magnification: ×200. (Scale bars, 50 μm.)

whereas only 10% of distal tip cells express the protein (Fig. 2*B*). There is nearly a 3-fold enrichment of Sca-1$^+$ cells in proximal vs. distal prostate tissue, and this is remarkably similar to the percentage of BrdUrd label-retaining cells (25%) in the proximal region reported by Tsujimura *et al.* (21). The percentage of cells expressing other markers, such as CD24, did not differ in each prostatic region (data not shown).

Immunofluorescent staining of longitudinal sections prepared from prostate from 8-week-old C57BL/6 mice indicates that the Sca-1 protein is expressed predominantly by epithelial cells in the proximal regions of prostatic tubules (Fig. 2*C Left*) and is relatively absent in cells at the distal tips (Fig. 2*C Right*). Some basement membrane and stromal cell staining is also present in each prostatic region (Fig. 2*C2*, white arrow) but is distinguishable from epithelial cell staining because it does not form the ring-like pattern typical of epithelial cell surface staining (Fig. 2*C3*, blue arrow).

To determine whether enrichment for prostate stem/progenitor cell elements after androgen ablation results in an increase in the percentage of Sca-1$^+$ cells, 8-week-old C57BL/6 mice were castrated, and dissociated cell suspensions were prepared 2 weeks later from these animals as well as age-matched controls. FACS analysis demonstrates that the percentage of Sca-1$^+$ cells is increased 6-fold in prostate tissue from castrated mice as compared with intact mice (Fig. 2*D*), indicating that the Sca-1 surface antigen is expressed on androgen-independent prostate stem/progenitor cells.

Increased Expression of Activated Akt1 in PRCs Is Sufficient for Prostate Cancer Initiation. Perturbations in the PTEN/AKT signaling axis are strongly correlated with prostate cancer development (22–26). To determine whether PRCs can be transformed and initiate prostate tumorigenesis, we investigated whether prostate cells infected with lentivirus containing a constitutively active form of AKT would regenerate cancerous tissue grafts in the regeneration system.

Dissociated prostate cells (1×10^5) from 8-week-old C57BL/6 mice were infected with lentivirus mediating the expression of constitutively active AKT1 or control lentivirus expressing only GFP (Fig. 6, which is published as supporting information on the PNAS web site). Each sample was mixed with 1×10^5 uninfected prostate cells and UGSM cells and was incubated under the kidney capsule of SCID mice for 8–10 weeks. Transillumination and fluorescence images show that grafts regenerated from AKT1 lentivirus-infected cells are much larger than control grafts (Fig. 3*A Left*). Grafts from AKT1 lentivirus-infected cells also appear

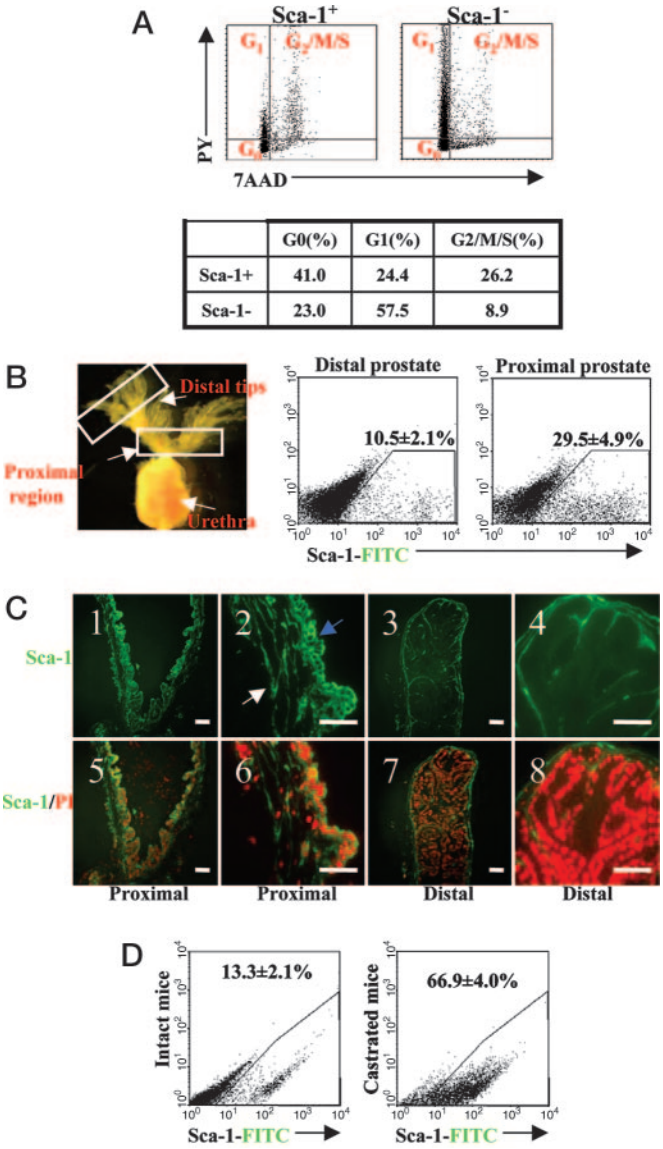

	G0(%)	G1(%)	G2/M/S(%)
Sca-1+	41.0	24.4	26.2
Sca-1-	23.0	57.5	8.9

Fig. 2. Sca-1$^+$ prostate cell fractions contain increased numbers of replication-quiescent, androgen-independent cells that cluster in the proximal region of murine prostatic tubules. (*A*) FACS analysis of cell cycle status of Sca-1$^+$ and Sca-1$^-$ cell fractions. Dissociated prostate cells from C57BL/6 mice were separated into Sca-1$^+$ and Sca-1$^-$ fractions by using magnetic beads. Each fraction was stained and analyzed by FACS for simultaneous quantification of DNA and RNA content as described in *Materials and Methods*. (*B*) FACS analysis of Sca-1 expression in alternative regions of the murine prostate. The proximal and distal regions of prostatic ducts from 8-week-old C57BL/6 mice were microdissected as shown. Dissociated cells from each region were stained with antibody against the Sca-1 antigen and compared by FACS. (*C*) Immunofluorescent analysis of Sca-1 expression. Longitudinal prostate tissue sections were stained with antibody against Sca-1 as described in *Materials and Methods*. Fluorescence microscopy images show the expression of Sca-1 in the proximal and distal regions of the murine prostate. Sections were counterstained with PI (red). Original magnification: *1*, *3*, *5*, and *7*, ×100; *2*, *4*, *6*, and *8*, ×200. (Scale bars: *1*, *3*, *5*, and *7*, 100 μm; *2*, *4*, *6*, and *8*, 50 μm.) (*D*) Sca-1-positive cells are enriched in prostate tissue from castrated mice. Cells were dissociated from the prostate tissue of 10-week-old castrated and intact C57BL/6 mice. FACS analysis of Sca-1 expression was performed by using a FITC-conjugated anti-Sca-1 antibody.

denser and less translucent than control grafts and display extensive angiogenesis (Fig. 3*A Lower Left*, blue arrow). The presence of GFP signal in regenerated tissues confirms that prostate cells were successfully infected by each lentivirus (Fig. 3*A*).

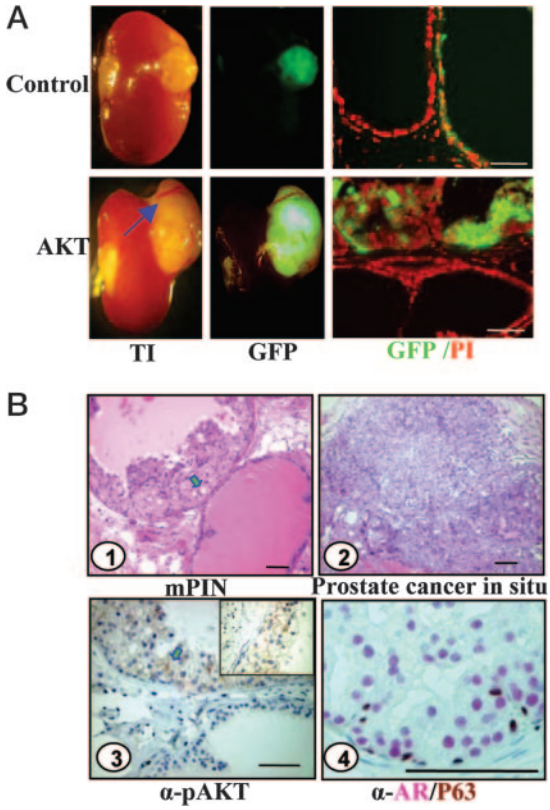

Fig. 3. Expression of constitutively active AKT1 in PRCs is sufficient to initiate tumorigenesis in the regeneration system. (*A*) Transillumination (TI) and fluorescent (GFP) microscopy analysis of grafts regenerated from prostate cells infected by control (*Upper*) or AKT1 (*Lower*) lentivirus. A blue arrow indicates sites of extensive angiogenesis. Frozen sections from each graft were counterstained with PI (GFP/PI) and analyzed by fluorescence microscopy. Original magnification: ×100. (Scale bars, 100 μm.) (*B*) (*1*) Histological and immunohistochemical analysis of tissue regenerated from cells infected by AKT1 lentivirus. (*2*) H&E staining of mPIN lesion (green arrow) and adenocarcinoma. (*3*) Phosphorylated AKT1 is only present in mPIN lesions (green arrow). (*Inset*) Clear plasma membrane staining characteristic of phospho-Akt1. (*4*) Immunohistochemical analysis of AR (red) and p63 (brown) within mPIN lesions. Original magnification: *1* and *2*, ×100; *3* and *4*, ×200; *Inset*, ×400. (Scale bars, 100 μm.)

Tissues regenerated from cells infected with the AKT1 lentivirus contain both normal and cancerous tissue structures. The histological severity in these grafts varies depending on the multiplicity of infection (moi) applied. Fig. 3*A* shows transilluminating and fluorescent images of representative grafts regenerated from cells infected with control or AKT1 lentivirus at high moi. Tissue sections of grafts regenerated from AKT1-infected cells show mouse PIN (mPIN) lesions when infected at low moi (moi = 5–10; Fig. 3*B1*) and fully developed carcinoma *in situ* when infected at high moi (moi > 20; Fig. 3*B2*) (27).

Immunohistochemical analysis demonstrates that activated AKT1 is expressed within cancerous tissue, confirming that such tubules are derived from AKT1 lentivirus-infected cells (Fig. 3*B3*). PIN lesions within each regenerated graft contain both AR$^+$ luminal cells (red) and p63$^+$ basal cells (brown) (Fig. 3*B4*). The presence of both cell types in regenerated PIN lesions suggests that the lesions are derived from cells that possess the capacity for multilineage differentiation. Areas of adenocarcinoma do not appear to contain p63$^+$ cells (data not shown). Experiments in which lentivirus containing small interfering RNA were used to knock down the expression of PTEN in dissociated prostate cells yielded similar results (Fig. 6).

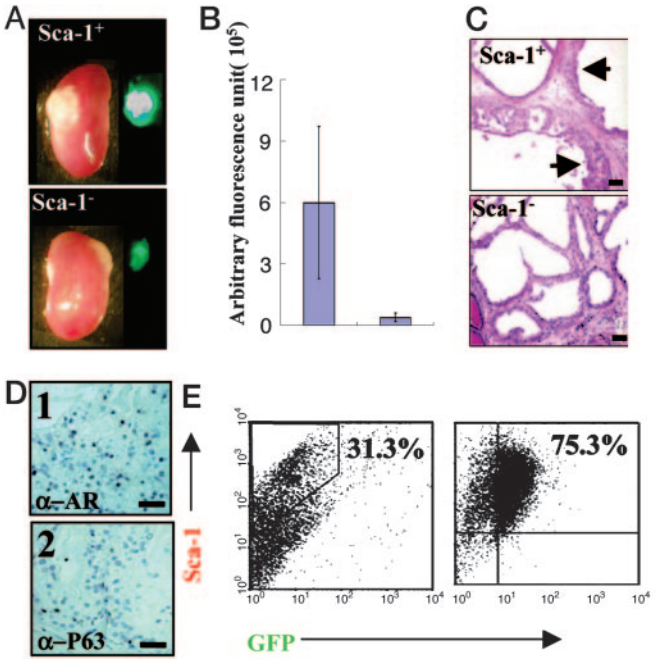

Fig. 4. Enrichment of PRCs by using the Sca-1 marker confirms the oncogenic potential of PRCs. (*A*) Regeneration of AKT1 lentivirus-infected Sca-1$^+$ and Sca-1$^-$ prostate epithelial cells. Cells from 8-week-old C57BL/6 mouse prostate tissue were separated into Sca-1$^+$ and Sca-1$^-$ fractions by using magnetic bead sorting and infected with AKT1 lentivirus. Infected Sca-1$^+$ or Sca-1$^-$ cells (5×10^4) were mixed with 1×10^5 UGSM cells and implanted under the kidney capsule of SCID mice. Regenerated grafts were harvested after a 6-week incubation and analyzed by transillumination and fluorescence microscopy. (*B*) Bar graph comparing the fluorescence signal emitted from each graft measured by a charge-coupled device camera. (*C*) Histological analyses of regenerated cancer tissue grafts. H&E staining shows mPIN lesions in sections from Sca-1$^+$ grafts (*Upper*) and normal tubular structures in sections from Sca-1$^-$ grafts (*Lower*). (*D*) Immunohistochemical staining for AR and p63 on representative sections from Sca-1$^+$ grafts. (Scale bars, 50 μm.) (*E*) Prostate cancer tissues contain increased percentages of Sca-1$^+$ cells. Dissociated cells from 8-week-old murine prostate tissue were infected with AKT1 lentivirus and incubated under the kidney capsule of SCID mice for 10 weeks. FACS analysis was performed on cells stained with a phycoerythrin-conjugated antibody against Sca-1.

Dissociated prostate cells from C57BL/6 mice were separated into Sca-1$^+$ and Sca-1$^-$ fractions by using magnetic bead sorting. Cells (5×10^4) from each fraction were infected with the AKT1 lentivirus, mixed with 1×10^5 UGSM cells, and incubated under the kidney capsule of SCID mice for 6 weeks. Transillumination and fluorescent images of representative grafts show that grafts regenerated from Sca-1$^+$ fractions are significantly larger than Sca-1$^-$ cell grafts (Fig. 4*A*). Quantification of GFP signal by a charge-coupled device camera demonstrates that grafts regenerated from Sca-1$^+$ cells contain 5- to 6-fold more fluorescence, and therefore more GFP$^+$ cells, than Sca-1$^-$ grafts (Fig. 4*B*).

Histological analysis of grafts regenerated from Sca-1-enriched PRCs show the presence of PIN lesions (Fig. 4*C*, black arrows). Normal tubule structures are also present in Sca-1$^+$ grafts (Fig. 4*C*, red arrow) but do not appear GFP$^+$, suggesting that they were not infected by lentivirus to produce atypical growth. Sca-1$^-$ grafts are predominantly composed of normal tubules, but a few tubules with cancerous lesions are present in Sca-1$^-$ grafts (Fig. 4*C*). Immunohistochemical analysis shows that cancerous tissue regenerated from Sca-1$^+$ cells contains both p63$^+$ basal cells and AR$^+$ luminal cells (Fig. 4*D*). Although Sca-1$^+$ and Sca-1$^-$ cells were not purified to homogeneity by using this technique, the enrichment of both prostate-regenerative and tumorigenic activity in Sca-1$^+$ fractions provides correlative evidence that PRCs can be efficiently transformed by single oncogenic perturbations to initiate prostate tumorigenesis.

Expression of the Wnt-1 proto-oncogene in the mammary gland of transgenic mice results in the expansion of epithelial cells expressing stem/progenitor cell markers such as keratin 6 and Sca-1, suggesting that mammary gland progenitor cells may be the targets for oncogenesis by Wnt-1 signaling elements (28). Single cell suspensions were prepared from prostatic tumor tissue regenerated from cells infected with the AKT1 lentivirus and from normal tissue regenerated from cells infected with control lentivirus. The majority of regenerated cancer cells are weakly GFP$^+$, as expected due to lentiviral infection. Interestingly, $\approx$75% of cells within these regenerated tissue grafts are Sca-1$^+$, and nearly all transformed cells (GFP$^+$) are Sca-1$^+$ (Fig. 4*E*). Only $\approx$30% of cells in the regenerated normal tissue are Sca-1$^+$ (Fig. 4*E*). Isotype controls for each tissue show negligible background (data not shown).

Discussion

Tissue stem cells are defined by their increased proliferative potential and capacity for multilineage differentiation and long-term self-renewal. Richardson *et al.* (29) recently reported that CD133$^+$ human prostate epithelial cells restricted to the integrin $\alpha_2\beta_1^{hi}$ subpopulation possess a high *in vitro* proliferative potential and can reconstitute prostatic-like acini *in vivo*. We demonstrate that the Sca-1 surface antigen can be used to enrich for murine prostate cells displaying multiple properties of primitive cells, including androgen independence, replication quiescence, multilineage differentiation, and *in vivo* prostate regenerative capacity. Additionally, we show that introduction of constitutively active AKT in Sca-1-enriched PRCs results in the initiation of prostate tumorigenesis and that prostate cancer progression correlates with an increase in the percentage of Sca-1$^+$ cells.

A hierarchical organization for differentiation has been proposed for the epithelial cell lineages that make up the prostate. Stem cells in the basal cell layer are thought to give rise to highly proliferative progenitor cells or TACs that differentiate to produce terminally differentiated, nonproliferative secretory luminal cells (10). FACS analysis demonstrating that Sca-1$^+$ cell fractions are enriched for G_0 cells indicates that the Sca-1$^+$ PRC subpopulation contains a population of stem-like cells. However, several lines of evidence suggest that the Sca-1$^+$ subpopulation is heterogeneous. First, the Sca-1$^+$ fraction is too large to be composed entirely of stem cells. Also, immunostaining shows that a subset of stromal cells may be Sca-1$^+$. The increased percentage of cycling cells in Sca-1$^+$ fractions suggests that this subpopulation may also include proliferative TACs. The fact that such a large percentage (70%) of prostate cells in tissue from castrated animals are Sca-1$^+$ further supports the presence of TACs in the Sca-1$^+$ subset because castrated tissue is known to contain both stem cells and TACs. These conclusions correspond with previous studies reporting that the Sca-1$^+$ bone marrow cell fraction includes long-term hematopoietic stem cells as well as more actively dividing short-term stem cells and progenitors that regularly enter the cell cycle (30, 31).

The presence of Sca-1 on the surface of murine hematopoietic, mammary, and putative prostate stem/progenitor cells implies there may be a conservation of this protein on tissue stem cells throughout development. Sca-1 is located on chromosome 15 in a multigene cluster of $\approx$18 highly conserved genes, including other known members such as prostate stem cell antigen (PSCA) and stem cell antigen-2 (32). PSCA and Sca-1 possess a number of interesting relationships. The proteins appear to display distinct expression patterns. Although Sca-1$^+$ cells localize to the proximal region, PSCA$^+$ are predominantly located in the distal tip cells of the murine prostate (33). Previous reports demonstrate that PSCA is up-regulated in both androgen-independent and androgen-dependent prostate cancer xenografts (34). In

addition to regenerated prostate cancer tissue, a dramatic increase in the percentage of Sca-1^+ cells has been found in cancerous tissue from transgenic animals with a prostate-specific conditional knockout of PTEN or overexpression of the c-myc oncogene (H. Wu and C. Sawyers, personal communications) (25, 35). The functional significance of the overexpression of these genes in prostate cancer remains to be determined.

We thank Alan Chin for technical support; Donghui Chen for FACS analysis; George V. Thomas in the Department of Pathology at University of California, Los Angeles (UCLA), for reviewing the histology of the regenerated tissues; and Caius Radu for helpful suggestions. We also thank Hong Wu and Charles Sawyers for permission to cite unpublished data. This work was supported by funds from the Prostate Cancer Foundation, UCLA Specialized Program of Research Excellence in Prostate Cancer (Jean Dekernion, Principal Investigator), and the Department of Urology at UCLA. O.N.W. is an Investigator of the Howard Hughes Medical Institute. D.A.L. is supported by National Institutes of Health Tumor Cell Biology Training Grant PHS T32 CA09056.

1. Reya, T., Morrison, S. J., Clarke, M. F. & Weissman, I. L. (2001) *Nature* **414,** 105–111.
2. Tu, S. M., Lin, S. H. & Logothetis, C. J. (2002) *Lancet Oncol.* **3,** 508–513.
3. Taipale, J. & Beachy, P. A. (2001) *Nature* **411,** 349–354.
4. Reya, T., Duncan, A. W., Ailles, L., Domen, J., Scherer, D. C., Willert, K., Hintz, L., Nusse, R. & Weissman, I. L. (2003) *Nature* **423,** 409–414.
5. Al-Hajj, M., Wicha, M. S., Benito-Hernandez, A., Morrison, S. J. & Clarke, M. F. (2003) *Proc. Natl. Acad. Sci. USA* **100,** 3983–3988.
6. Lapidot, T., Sirard, C., Vormoor, J., Murdoch, B., Hoang, T., Caceres-Cortes, J., Minden, M., Paterson, B., Caligiuri, M. A. & Dick, J. E. (1994) *Nature* **367,** 645–648.
7. Singh, S. K., Hawkins, C., Clarke, I. D., Squire, J. A., Bayani, J., Hide, T., Henkelman, R. M., Cusimano, M. D. & Dirks, P. B. (2004) *Nature* **432,** 396–401.
8. Foster, C. S., Dodson, A., Karavana, V., Smith, P. H. & Ke, Y. (2002) *J. Pathol.* **197,** 551–565.
9. Abate-Shen, C. & Shen, M. M. (2000) *Genes Dev.* **14,** 2410–2434.
10. Uzgare, A. R., Xu, Y. & Isaacs, J. T. (2004) *J. Cell Biochem.* **91,** 196–205.
11. Isaacs, J. T. (1985) in *Benign Prostatic Hyperplasia*, eds. Rodgers, C. H., Coffey, D. S. & Cunha, G. R. (National Institutes of Health, Washington, D.C.), pp. 85–94.
12. Verhagen, A. P., Ramaekers, F. C., Aalders, T. W., Schaafsma, H. E., Debruyne, F. M. & Schalken, J. A. (1992) *Cancer Res.* **52,** 6182–6187.
13. Signoretti, S., Waltregny, D., Dilks, J., Isaac, B., Lin, D., Garraway, L., Yang, A., Montironi, R., McKeon, F. & Loda, M. (2000) *Am. J. Pathol.* **157,** 1769–1775.
14. De Marzo, A. M., Meeker, A. K., Epstein, J. I. & Coffey, D. S. (1998) *Am. J. Pathol.* **153,** 911–919.
15. Litvinov, I. V., De Marzo, A. M. & Isaacs, J. T. (2003) *J. Clin. Endocrinol. Metab.* **88,** 2972–2982.
16. Cunha, G. R. & Lung, B. (1978) *J. Exp. Zool.* **205,** 181–193.
17. Xin, L., Ide, H., Kim, Y., Dubey, P. & Witte, O. N. (2003) *Proc. Natl. Acad. Sci. USA* **100,** Suppl. 1, 11896–11903.
18. Spangrude, G. J., Heimfeld, S. & Weissman, I. L. (1988) *Science* **241,** 58–62.
19. Welm, B. E., Tepera, S. B., Venezia, T., Graubert, T. A., Rosen, J. M. & Goodell, M. A. (2002) *Dev. Biol.* **245,** 42–56.
20. Schmid, I., Cole, S. W., Korin, Y. D., Zack, J. A. & Giorgi, J. V. (2000) *Cytometry* **39,** 108–116.
21. Tsujimura, A., Koikawa, Y., Salm, S., Takao, T., Coetzee, S., Moscatelli, D., Shapiro, E., Lepor, H., Sun, T. T. & Wilson, E. L. (2002) *J. Cell Biol.* **157,** 1257–1265.
22. DeMarzo, A. M., Nelson, W. G., Isaacs, W. B. & Epstein, J. I. (2003) *Lancet* **361,** 955–964.
23. Vivanco, I. & Sawyers, C. L. (2002) *Nat. Rev. Cancer* **2,** 489–501.
24. Backman, S. A., Ghazarian, D., So, K., Sanchez, O., Wagner, K. U., Hennighausen, L., Suzuki, A., Tsao, M. S., Chapman, W. B., Stambolic, V. & Mak, T. W. (2004) *Proc. Natl. Acad. Sci. USA* **101,** 1725–1730.
25. Wang, S., Gao, J., Lei, Q., Rozengurt, N., Pritchard, C., Jiao, J., Thomas, G. V., Li, G., Roy-Burman, P., Nelson, P. S., *et al.* (2003) *Cancer Cell* **4,** 209–221.
26. Majumder, P. K., Yeh, J. J., George, D. J., Febbo, P. G., Kum, J., Xue, Q., Bikoff, R., Ma, H., Kantoff, P. W., Golub, T. R., *et al.* (2003) *Proc. Natl. Acad. Sci. USA* **100,** 7841–7846.
27. Shappell, S. B., Thomas, G. V., Roberts, R. L., Herbert, R., Ittmann, M. M., Rubin, M. A., Humphrey, P. A., Sundberg, J. P., Rozengurt, N., Barrios, R., *et al.* (2004) *Cancer Res.* **64,** 2270–2305.
28. Li, Y., Welm, B., Podsypanina, K., Huang, S., Chamorro, M., Zhang, X., Rowlands, T., Egeblad, M., Cowin, P., Werb, Z., *et al.* (2003) *Proc. Natl. Acad. Sci. USA* **100,** 15853–15858.
29. Richardson, G. D., Robson, C. N., Lang, S. H., Neal, D. E., Maitland, N. J. & Collins, A. T. (2004) *J. Cell Sci.* **117,** 3539–3545.
30. Morrison, S. J., Wandycz, A. M., Hemmati, H. D., Wright, D. E. & Weissman, I. L. (1997) *Development (Cambridge, U.K.)* **124,** 1929–1939.
31. Cheshier, S. H., Morrison, S. J., Liao, X. & Weissman, I. L. (1999) *Proc. Natl. Acad. Sci. USA* **96,** 3120–3125.
32. Gumley, T. P., McKenzie, I. F. & Sandrin, M. S. (1995) *Immunol. Cell Biol.* **73,** 277–296.
33. Watabe, T., Lin, M., Ide, H., Donjacour, A. A., Cunha, G. R., Witte, O. N. & Reiter, R. E. (2002) *Proc. Natl. Acad. Sci. USA* **99,** 401–406.
34. Reiter, R. E., Gu, Z., Watabe, T., Thomas, G., Szigeti, K., Davis, E., Wahl, M., Nisitani, S., Yamashiro, J., Le Beau, M. M., *et al.* (1998) *Proc. Natl. Acad. Sci. USA* **95,** 1735–1740.
35. Ellwood-Yen, K., Graeber, T. G., Wongvipat, J., Iruela-Arispe, M. L., Zhang, J., Matusik, R., Thomas, G. V. & Sawyers, C. L. (2003) *Cancer Cell* **4,** 223–238.